Journal of Asian Concrete Federation
Vol. 11, No. 2, pp. 81-100, June 2025
ISSN 2465-7964/ eISSN 2465-7972
DOI http://dx.doi.org/10.18702/acf.2025.11.2.81

Review Paper

Binder jetting 3D printing in civil engineering: materials, process optimization, and structural applications

Tingyu Hu, Zhijian Li, Guowei Ma*

(Received: 21-Apr-2025; Revised: 08-Jun-2025; Accepted: 09-Jun-2025; Published online: 25-Jun-2025)

Abstract: Binder jetting 3D printing (BJ3DP) underscores the frontier of additive manufacturing in civil engineering due to diverse applications, high precision and high cost-effectiveness. It is especially acclaimed for its viability to produce delicate interior architectures and suspension elements, such as thin-shell structures and hollow structures, without engagement of support or mold. This review systematically synthesizes the current research landscape of BJ3DP in civil engineering, with a focus on the fundamental principles governing the implementation process, especially for fabrication of complex geometries with interior architecture, pertaining to material compatibility, optimization of process parameters, enhancement of structural performance. The review also addresses existing technological limitations and proposes avenues for future research. Furthermore, BJ3DP has demonstrated successful application in the customized fabrication of architectural ornamentation, geological models, and lightweight structural elements. Nevertheless, practical engineering applications of BJ3DP in civil engineering is hindered by several challenges. Future research endeavors should prioritize investigations into multi-material compatibility, the development of intelligent process control methodologies, and the establishment of a comprehensive framework for performance evaluation to facilitate practical engineering application of BJ3DP in automation construction.

Keywords: Binder jetting 3D printing; Material parameters; Process parameters; Post-processing

1. Introduction

3D printing (3DP), also known as additive manufacturing (AM), originated in the 1980s, is an advanced fabrication technique based on the principle of layer-by-layer deposition [1-3]. This technology has revolutionized traditional manufacturing processes by enabling mold-free, high-precision production of complex geometries with automation, flexibility, and digital intelligence [4-6].

Currently, 3DP technology has been extensively adopted across multiple industries, including aerospace, healthcare, automotive manufacturing, and consumer electronics [7-9]. In the medical field, bioprinting technology has been successfully implemented to fabricate patient-specific prostheses and orthodontic devices. The aerospace industry has adopted titanium alloy-based laser powder bed fusion (LPBF) techniques to manufacture structural components with optimized strength-to-weight ratios. Automotive manufacturers leverage 3DP for rapid prototyping of complex exterior geometries, enabling accelerated design iteration cycles. Additionally, 3DP has become a global research hotspot in intelligent construction technology [10-12]. These successful implementations underscore the significant potential of 3DP in driving innovation and industrial advancement.

Among the various 3DP techniques, extrusion-based

*Corresponding author **Guowei Ma,** *School of Civil and Transportation Engineering, Hebei University of Technology, Tianjin 300401, China. E-mail: guowei.ma@hebut.edu.cn*
Tingyu Hu, *School of Civil and Transportation Engineering, Hebei University of Technology, Tianjin 300401, China. E-mail: 409008950@qq.com*
Zhijian Li, *School of Civil and Transportation Engineering, Hebei University of Technology, Tianjin 300401, China. E-mail: zhijian.li@hebut.edu.cn*

3D printing and binder jetting 3D printing (BJ3DP) are widely used in civil engineering [13, 14]. Compared to extrusion-based 3D printing, BJ3DP has gained significant research interest in civil engineering owing to high precision, broad material adaptability and capability to fabricate complex overhang structures without additional support [15-17]. The technology selectively sprays and deposits liquid binder onto powder bed, bonding particles to form solid structures in a layer-by-layer fashion [18-20]. Compared with other 3DP techniques, BJ3DP demonstrates distinctive advantages including high productivity, material versatility and efficiency, low energy consumption, and scalability [21-23]. A variety of materials, such as gypsum, cementitious composites, ceramics, and quartz sand, can be employed, enabling applications in architectural components, formworks production, artificial rock models and functional infrastructure development [24, 25]. Fig. 1 is the printing schematic diagram of BJ3DP

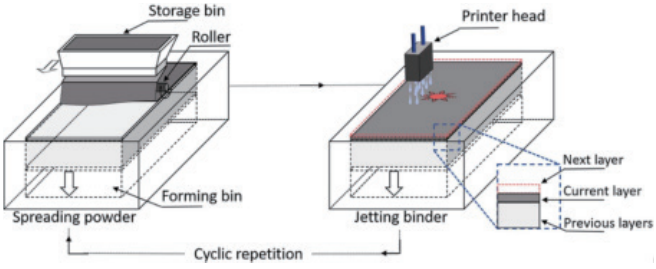

Fig. 1. Schematic flowchart of BJ3DP process [3].

Application of BJ3DP in civil engineering has progressed significantly through ongoing technological developments in material systems, powder bed preparation methods, binder formulations, and processing parameter optimization [26-28]. In July 2008, the first attempt to print a conglomerate structure (The Radiolaria Pavillon) was carried out in Buti (Italy) [29]. Another example of object form differentiation is the optimized permanent template, and the resulting geometric shapes are difficult to manufacture using traditional manufacturing techniques [30]. More than 150 individual template elements for a 12 × 8-meter concrete ceiling were 3D-printed. The printed templates enabled the optimization of free geometric shapes and complex geometric features on the surface. The shape and layout of the printed templates were optimized to reduce material usage and minimize warping. Compared with traditional large-scale designs, the weight was reduced from 45 tons to approximately 15 tons [29]. Experimental evidences have shown printability and performance of BJ3DP components are influenced by multiple key factors, including powder particle size and morphology, flowability, binder saturation, printing layer thickness, printing orientation, and post-processing techniques [31-34]. These factors directly affect the mechanical strength, dimensional accuracy, porosity, and overall durability of printed specimens.

This review presents a comprehensive evaluation of BJ3DP in civil engineering, systematically analyzing material classifications, printing parameters, post-processing methods, implementation case studies, and technological limitations, while highlighting future research directions. The objective is to provide comprehensive and actionable insights for researchers and practitioners committed to developing intelligent and sustainable construction technologies via the implementation of BJ3DP.

2. Materials selection

Selection of materials is crucial for binder jetting 3D printing (BJ3DP) technology. Properties of build powder materials, such as particle size, particle morphology, and flowability, can significantly affect powder spreading performance, printing accuracy, and mechanical properties. Based on BJ3DP technology, researchers have developed various types of 3D printing systems tailored to different printing materials, including gypsum-based BJ3DP [35], cement-based BJ3DP [27], ceramic-based BJ3DP [1], and sand-based BJ3DP [36],as shown in Table 1.

The powder morphology significantly influences the processability in BJ3DP, and spherical powders are preferred due to their ability to achieve higher powder bed density [37]. Although powder morphology shows the visual structure of powder material, particle size distribution (PSD) is usually used to quantify the size of powder. PSD affects the fluidity of powder, the spreading of powder bed, and porosity. Zhou et al. [38] demonstrated that PSD affects the uniformity of powder

bed density, thereby changing the permeability of binder. Uneven particle distribution prolongs the binder penetration time, while fine particle aggregation creates macroscopic voids, compromising wetting efficiency. Powder fluidity is an important factor in BJ3DP, as it influences the spreading performance of powder on the printing platform. Sufficient fluidity enables the formation of thin and uniform powder layers via roller or blade spreading, which is critical for achieving high printing resolution, dimensional accuracy, and specimen density. Conversely, insufficient fluidity causes uneven powder bed deposition and surface irregularities. Schade et al. [39] research showed that there is an inverse relationship between powder fluidity and particle size. Chen et al. [40] reported that powder fluidity improves when particle radius exceeds 21.8 μm, improving the quality of powder bed. Below this threshold, increased van der Waals forces between particles reduce fluidity and compromise spreading performance. Therefore, as the van der Waals force between the particles increases, the fluidity of fine powder is usually less than that of coarse powder. Although BJ3DP typically employs fine powders (tens to hundreds of micrometers) to match layer thickness requirements, excessive fineness compromises fluidity and spreading performance. Thus, modification of powder properties is essential for optimizing bed quality and printing precision.

Table 1. Comparison of common materials for binder jetting 3D printing.

Material Type	Physical Properties	Mechanical Characteristics	Applicable Range	Pros	Cons
Gypsum	Fine, white powder, porous	Low to medium compressive strength; brittle; low tensile strength; moderate hardness	Art sculptures, dental molds, architectural models	Easy to process, good detail, low cost	Low water resistance, lower mechanical strength
Cementitious/ geopolymer materials	Powder, hardens when mixed with water	Moderate compressive strength; brittle; low tensile strength; some flexibility	Construction molds, architectural components	Widely available, inexpensive	Slow curing, surface roughness, susceptible to cracking
Ceramic	High melting points, ceramic nature	High hardness and compressive strength; low tensile strength; brittle failure; excellent wear resistance	Dental, aerospace, electronic components	Excellent heat resistance, high temperature stability	Fragility, post-processing requirements
Sand	High density, granular, inert	Moderate compressive strength, low fracture toughness, coarse surface	Architectural models, molds, casting patterns	Low cost, good resolution, wide availability	Limited mechanical strength, surface roughness

2.1. Gypsum

Gypsum is an air-hardening cementitious material, primarily composing of natural gypsum and industrial by-product gypsum. Natural gypsum consists of calcium sulfate dihydrate ($CaSO_4 \cdot 2H_2O$) with density of 2.96 g/cm³. Most gypsum materials used in BJ3DP are mainly composed of calcium sulfate hemihydrate ($CaSO_4 \cdot 0.5H_2O$), with density ranging from 2.6 to 2.7 g/cm³ [41, 42]. Gypsum powder demonstrates excellent processability and high compatibility with BJ3DP technology. Since particle size can be adjusted according to specific product requirements, it avails fine and precise printing. Moreover, white color of gypsum powder facilitates full-color printing capabilities, which allows for enhanced reproduction of model details. These advantages have garnered significant attention from researchers exploring BJ3DP gypsum materials.

The reaction mechanism of gypsum-based cementitious materials is the hydration process, in which calcium sulfate hemihydrate converts into calcium sulfate dihydrate upon contact with water, ultimately consolidating to confer certain strength. Specifically, when gypsum is mixed with water, it dissolves in the liquid phase, increasing the concentrations of calcium and sulfate ions. When the ion concentration reaches critical supersaturation level, dihydrate gypsum nuclei begin to form. As the hydration of hemihydrate gypsum progresses, more dihydrate gypsum crystals form and grow, gradually interlocking into a crystalline network that contributes to the material's strength development.

A number of studies have been reported on gypsum-

based BJ3DP specimens. Specifically, Ma et al.[43] improved the powder spreading performance of gypsum by incorporating hydrophobic silica. By comparing the effects of different sizes and surface morphologies of silica particles on flowability and spreading quality of gypsum, they found that adding 1 wt% hydrophobic nano-silica resulted in optimal flowability and spreading performance. Additionally, gypsum 3D printing has gained significant attention in the field of rock engineering. Kong et al.[44, 45] utilized X-ray computed tomography (X-CT) and scanning electron microscopy (SEM) to investigate the mechanical and pore structure of gypsum-based BJ3DP specimens. Surface porosity of 5.8% and total porosity of 21% in the printed specimens have been achieved. Additionally, the internal pores of the samples were predominantly spherical without exhibition of blade-like cracks. It suggests that this material is suitable for fabrication of lightweight artificial rocks or masonry. Jiang et al. [46] also used gypsum powder to print rock models with internal voids and pre-existing cracks. Mechanical testing under uniaxial compression demonstrated that the mechanical properties of 3D printed rock specimens closely resembled those of natural rock counterparts.

2.2. Cementitious/geopolymer materials

In recent years, cement-based BJ3DP has attracted significant attention in variable areas such as architectural decoration and customized fine structures. Cement-based materials undergo hydration reaction upon contact with the binder, bonding and hardening in designated areas to form target objects. This process imposes high requirements on the properties of the cement build materials. Specifically, cement-based materials for BJ3DP should exhibit good flowability and high hydration rate.

Xia et al. [47] developed 3D printed geopolymers catering for binder jetting 3D printing technology. The printability of the prepared geopolymer was quantitatively evaluated through powder bed spreading behavior, powder bed density, porosity, and binder droplet infiltration characteristics. It was found that increasing binder saturation significantly reduced the printing accuracy of the specimens, with the least dimensional error being observed along the Z-axis. Post-processing method for slag-based geopolymer materials commensurate BJ3DP was also proposed [48]. As shown in Fig. 2, BJ3DP technology achieved fabrication of intricate rectangular structures with minimum feature sizes of 1 mm. The dimensional accuracy, apparent porosity, and mechanical properties of the printed cubic specimens were evaluated and optimized. Post-treatment of immersion in sodium metasilicate solution at 60°C resulted in remarkable mechanical enhancement, increasing compressive strength from 0.91 MPa to 16.5 MPa. These studies provide valuable insights for approptiaye selection and optimization of cement-based materials for BJ3DP technology.

Different particle sizes, morphology, and flowability of cement powders influence powder spreading performance, powder bed density, and porosity. Additionally, the choice of binder can impact the mechanical properties and dimensional accuracy of printed specimens. Among the variety of cement-based materials suitable for BJ3DP, including calcium aluminate cement [49], magnesium phosphate cement (MPC) [26], Portland cement [50], and calcium sulfoaluminate cement [51]. MPC is particularly suited for BJ3DP for favor of rapid setting, early strength development, and excellent bonding properties. Ma et al. [27] developed a magnesium phosphate cement material tailored for BJ3DP, and conducted preliminary studies on printability and mechanical properties. The results showed that adding 25 wt% quartz sand significantly improved powder bed spreadability, while incorporating 5 wt% polyvinyl alcohol reduced the porosity of printed specimens by 2.86%. Application of cement-based materials in binder jetting 3D printing is gradually becoming mature, and various types of commercial cementitious powders have been developed. Shakor et al. [52] evaluated the mechanical properties of a cementitious powder composing mainly of 30.8% ordinary Portland cement, 64.7% calcium aluminate cement, and 4.5% lithium carbonate. With increasing binder saturation, the compressive strength of printed cube specimens improved, achieving 8.3 MPa after 28-day water curing.

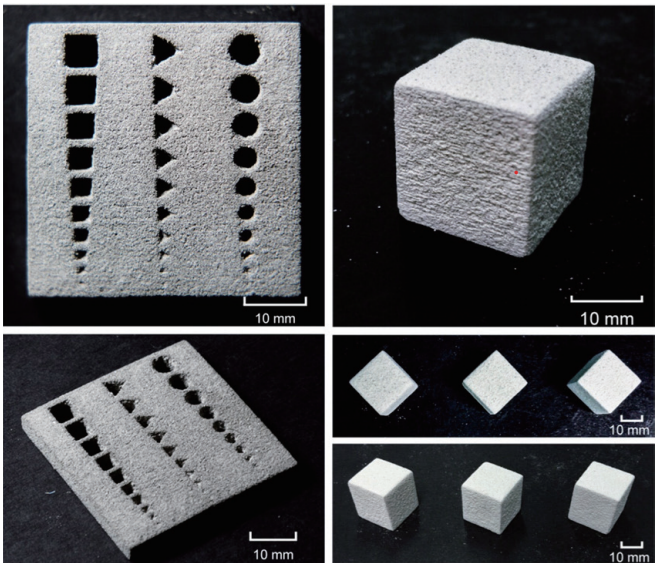

Fig. 2. Plate and cubic specimens with BJ3DP geopolymer material [48].

In conventional cast concrete materials, addition of well-graded aggregates not only reduces the amount of cement paste required, but also enhances the mechanical properties and durability of the casted concrete. However, in binder jetting 3D printing processes, aggregate particle size is highly constrained by the thickness of the printing layer. When the particle size of powder is significantly larger than the layer thickness, the powder bed cannot be uniformly spread, the printing process fails to proceed smoothly. Joseph et al.[53] incorporated rounded silica sand as fine aggregate into calcium aluminate cement. The printing layer thickness was set at 0.152 mm. Sand particles with size marginally exceeding the layer height enhanced interlayer bonding. The specimens produced with this fine sand aggregate yielded density ranging from 1474-1501 kg/m³, alongside 28-day compressive strength of 5.94-6.70 MPa and flexural strength of 1.76-2.39 MPa.

Pegna [54] pioneered the concept of concrete component fabrication through additive manufacturing in 1995, proposing a novel approach of layer-by-layer selective deposition using Portland cement. This groundbreaking work successfully produced a hollow structural element measuring 7.6 × 7.6 × 15.2 cm³. So far, BJ3DP technology has also proven effective for producing large-scale structures [55]. For example, Rael et al. [29] used portland cement to print a pavilion measuring approximately 2.7 × 3.7 × 3.7 m³. The structure comprises 840 custom-printed components assembled into a cohesive delicate structure, as shown in Fig. 3.

Fig. 3. Binder jetting 3D printed gallery [29]

2.3. Ceramic

Conventional ceramic manufacturing predominantly relies on mold-dependent pressing techniques, which are generally time-consuming and costly. Ceramic-based 3D printing technology streamlines this process by eliminating the need for molds and complex manual procedures, thereby significantly reducing production costs and improving the efficiency of ceramic fabrication. Due to their excellent biocompatibility, durability, and mechanical properties, ceramics are widely used in fields of biomedical engineering and aerospace [56, 57]. Currently, prevailing ceramic materials include titanium silicon carbide ceramics, porous silicon nitride ceramics, alumina ceramics, and tricalcium phosphate ceramics. Amongst, the most representative are polymer-derived ceramics (PDCs), such as silicon carbide (SiC), silicon nitride (Si_4N_3), silicon oxycarbide (SiOC), and silicon carbonitride (SiCN), which can serve as raw build materials for 3D printing [58].

Teng et al. [59] developed BJ3DP ceramic powder formulation using zirconia as the base material and formulated matching binder for experimental validation. Du et al. [60] emphasized that the inherent brittleness,

elevated hardness, and high melting points of ceramics conferred challenges in identifying appropriate ceramic powders for binder jetting applications. The study focused on the effects of different layer thickness, powder particle quality, and post-processing methods on porosity and mechanical performance of printed materials. Among ceramic materials employed in binder jetting 3D printing, alumina (Al_2O_3) is one of the most widely utilized in 3D printing engine components, grinding tools, dental implants, and artificial bone prosthesis. Gonzalez et al. [61] utilized alumina powder to optimize parameters such as layer thickness, binder saturation, and particle size distribution. This optimization yielded printed parts with low porosity, achieving compressive strength as high as 131.86 MPa after 16 hours of sintering. Marczyk et al. [62] further adjusted particle size distribution using printing parameters of 0.12 mm layer thickness, 10 mm/s roller speed, and 80% binder saturation, successfully fabricating high-precision electronic components, as shown in the Fig. 4.

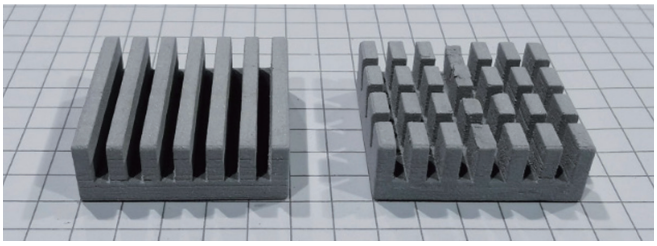

Fig. 4. Heat sinks by binder jetting technology using aluminum powder [62].

2.4. Quartz–sand

Sand is mainly classified into coated sand in selective laser sintering (SLS) and resin sand in binder jetting 3D printing (BJ3DP). Coated sand is a molding material to print casting cores or molds through SLS process. When combined with traditional casting techniques, this technology facilitates rapid production of metal components. Resin sand primarily includes silica sand, furan resin binders, and phenolic resin binders, which are used to build sand cores and molds via BJ3DP process. Coated sand exhibits excellent sintering performance, rendering it particularly suitable for the rapid casting of metal components with complex geometries. This technology is widely used in fields of aerospace and automotive manufacturing. In 2023, voxeljet presented a groundbreaking innovation: a new cold IOB (inorganic binding) 3D printing technology. With this unique process, molds and cores for the foundry industry can be produced from sand and an inorganic binder without the need for microwave treatment [63].

Companies like ExOne, Voxeljet, and ZCorp have utilized BJ3DP to produce sand molds using quartz sand and resin as printing materials. Compared to conventional sand-casting mold production, sand-based 3D printing technology simplifies the production process by eliminating the need for molds and core boxes, thereby substantially shortening product development timelines. The automated manufacturing process, being executed through computer-controlled systems, minimizes manual intervention while achieving millimeter-scale dimensional accuracy. By circumventing the conventional mold-making process, this method enhances design and manufacturing efficiency, and enables fabrication of molds with free-form surfaces and complex integrated components. It also eliminates mold-making errors and secondary deviations caused during replication, resulting in 50-80% reduction in new product development time [64]. Lorenzo et al. [65] fabricated standardized test specimens using furan resin binders and conducted test on compressive strength, flexural strength, and anisotropic mechanical properties. The cube specimens exhibited the highest compressive strength of 5.9 MPa in the Z-direction, while the rectangular specimens achieved the maximum flexural strength of 2.16 MPa. However, surface finish of binder-jetted sand molds remains inherently constrained by particulate morphology, necessitating additional surface finishing operations. Consequently, printing accuracy of sand-based 3D printed technology is yet to be improved.

3. Printing parameters

Binder jetting 3D printing system comprises several major components, i.e. the print head, build box, feed box, and roller, that work coordinately to fulfil the printing process. To accommodate diverse materials and binder formulations with distinct properties, each

subsystem requires precise parameter calibration to ensure optimal printing performance. The critical printing parameters include the particle size distribution and flowability for each ingredient of build materials, the binder's viscosity and surface tension, the printed head's traversal velocity and droplet ejection frequency, as well as the layer thickness and printing orientation.

3.1. Powder

The particle size distribution, surface roughness, particle shape, and hygroscopicity of powder materials can significantly influence powder deposition and spreading performance. Fine powders ensue enhanced packing density through minimizing void space, while generally exhibiting lower flowability due to high interparticle cohesion. Conversely, coarse powders confer better flowability and facilitate more homogeneous powder bed formation, albeit with increased interstitial porosity. The powder bed density directly affects diffusion and infiltration behavior of the binder, thereby impacting the dimensional accuracy and mechanical properties of printed specimens [66]. Butscher et al. [67] found that particle size distribution and powder flowability can affect the printability of the material. Their research results indicated that the powder material with average particle size of 20 to 35 μm, fluidity of 5 to 7, and powder bed surface roughness of 10 to 25 μm ensued the highest printing accuracy. Amir et al. [68] further demonstrated that, subject to identical printing parameters such as layer thickness, binder saturation, and drying time, the particle size distribution is a crucial factor in determining the dimensional accuracy, porosity, and microstructure.

3.2. Binder

The BJ3DP binders mainly include water-based binders and organic binders. Water-based binders are mainly used for powder materials such as cement and gypsum, while organic binders are mainly used for silica sand powder materials. The binder permeates and diffuses in the powder bed and bonds the loose powder, which largely determines the forming accuracy and mechanical properties of the printing component. Although the droplet size is not the exclusive factor affecting printing accuracy, smaller binder droplets combining with higher jetting frequency are generally more effective in reducing printing errors. Additionally, the binder droplet surface tension, viscosity, and saturation are crucial factors that influence droplet ejection, penetration and diffusion behaviors during the printing process.

Viscosity of binder is contingent upon its chemical compositions, molecular weight and the properties of the solvent. Viscosity affects the fluidity and jetting performance of the binder. Excessively high viscosity may incur nozzle clogging and reduce printing accuracy, while excessively low viscosity prevents the binder from effectively bonding the powder, negating the strength of printed specimen [69]. Surface tension mainly depends on the chemical compositions of the binder and contents of surfactants. For example, adding surfactants can reduce the surface tension and improve wetting performance. Surface tension governs spreading and wetting ability of the binder on the powder surface. Excessively high surface tension may prevent the binder from fully wetting the powder, resulting in uneven bonding layer, and thus negating the quality and strength of printed objects. Ma et al. [27] optimized binder properties by adding 5 wt% 1,2-propanediol and 0.1 wt% Surfynol 465 to deionized water, achieving surface tension of 38.4 mN/m and viscosity of 1.27 mPa·s, which improved penetration behavior and printing accuracy.

Binder saturation refers to the ratio of the amount of binder dispensed by the print head to the bonded build material volume. Improper binder saturation may lead to uneven build layer thickness, and thus dimensional inaccuracies in printed specimens. To produce green bodies with sufficient mechanical strength and surface quality, it is essential to optimize binder saturation. As shown in Fig. 5, both under-saturation and over-saturation increase powder bed surface roughness [70]. Low binder saturation results in incomplete curing of the powder material, and thus increasing pores and defects. Conversely, excessive saturation may cause excess powder particles to adhere to the surface of printed specimens. Another issue associated with over-saturation is excessive wetting of the powder bed, which may cause particles sticking to the roller. As

a result, the powder bed is not uniform, and cracks, roughness and even deviation exhibit in the powder bed [71].

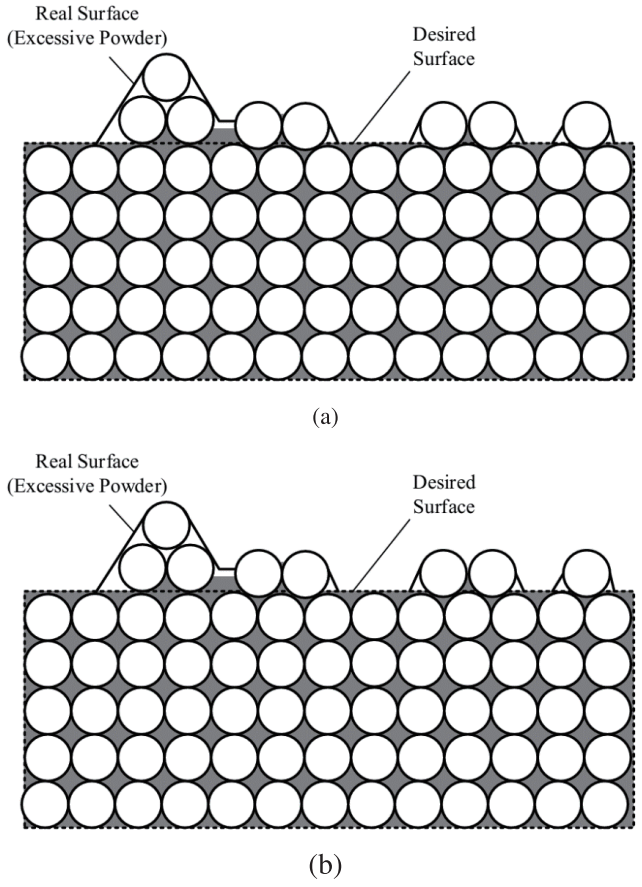

Fig. 5. Reduction of dimensional accuracy by improper saturation levels: (a) excessively low saturation and (b) over-high saturation [70].

3.3. Print speed

The powder spreading speed refers to the velocity at which the roller moves in the direction of powder spreading during the printing process. It directly affects the efficiency and uniformity of powder bed. Shrestha [72] tested spreading speeds ranging from 6 mm/s to 14 mm/s. The results indicated that speed of 6 mm/s achieved high printing accuracy. However, if the speed drops below 6 mm/s, although accuracy may improve further, the overall printing time increased substantially. Due to the combined effects of roller compaction and inter-particle interactions, the powder spreading process on the powder bed surface is complex, involving particle rotation, translation, and sliding motions. To achieve denser powder bed, roller movement and rotational speeds should be optimized through testing. The research by Shanjani et al. [73] indicated that rolling friction conditions, roller geometry, and the characteristics of loose powder affected the state of powder compaction, which in turn affected the density and mechanical properties of the green body and sintered components. As shown in Fig. 6, increasing the printing speed while maintaining a constant layer thickness results in reduced accuracy of the model in all directions. It is attributed to that the binder droplets are ejected from the nozzle and fall onto the powder bed surface along a parabolic trajectory [74]. Due to translational acceleration when the printhead starts and stops, lower printing speed cause the binder droplets to deviate from their intended path. Consequently, the printing accuracy in the printhead movement direction is generally lower than that in the powder spreading direction.

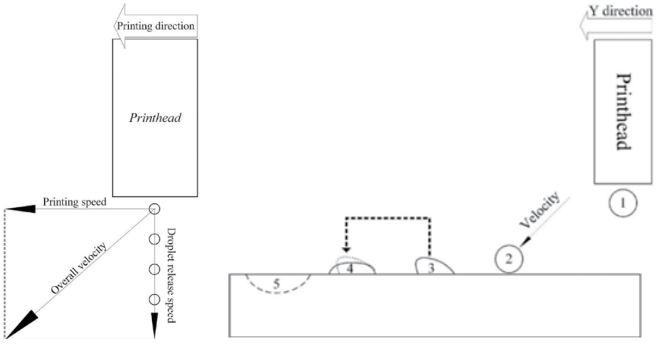

Fig. 6. Motion state of binder droplet (a) in-flight; (b) on the powder bed [74].

3.4. Layer thickness

In binder jetting 3D printing process, when the current layer is completed, the build platform descends a fixed distance to lay the powder material for the next layer. This fixed distance is termed as the layer thickness, which is one of the key parameters in BJ3DP. Typically, layer thickness ranges from 15 to 300 μm and should be calibrated before printing begins. Layer thickness directly affects the surface roughness

and dimensional accuracy of printed specimens. Lower layer thickness results in better surface quality and higher dimensional accuracy. However, excessively small layer thickness increases printing time, and thus compromises printing efficiency. Vaezi et al. [75] studied the impact of different layer thicknesses on the mechanical properties of 3D printed specimens. Under similar binder saturation conditions, increasing the layer thickness from 0.087 mm to 0.1 mm led to a decrease in tensile strength. This is because higher layer thickness increases the binder penetration distance between layers, resulting in decrease in the interlayer bonding strength. Layer thickness is also closely related to powder utilization rate and binder consumption. Thinner layer allows for more precise control of powder usage, improving material efficiency. In contrast, thicker layer reduces the number of binder jetting cycles required, but at stake that the binder may not penetrate completely the thick powder layer [48]. Additionally, powder flowability is also influenced by layer thickness. Thinner layer requires relatively higher powder flowability to ensure smooth and uniform spreading under the action of the roller. Simultaneously, powder particle size should be smaller than the layer thickness. In this regard, smaller particles tend to agglomerate, which hinders uniform spreading of powder [76].

3.5. Printing orientation

In binder jetting 3D printing process, it is essential to define the printing directions. The layer stacking direction is usually designated as the Z-direction, while the powder spreading direction and printhead movement direction are defined as the X- and Y-directions, respectively [26]. The printed model exhibits different pore distributions and mechanical properties in different printing directions. In other words, binder jetting 3D printed specimen exhibits anisotropy contingent upon the printing direction [26]. As shown in Fig. 7(a), Shao et al. [77] fabricated 3D printed gypsum-based rock-like specimens in different printing orientations, and investigated how printing direction and bedding plane affect anisotropy of printed specimens. The failure modes of rocks under different printing directions are different. Specimens with small inclination angle primarily exhibited shear failure, whereas those with large inclination angle ensued tensile failure. He et al. [78] found that printing direction significantly influenced the mechanical properties of 3D printed gypsum-based rock. As shown in Fig. 7(b), failure modes of cylindrical specimens under different printing directions are different. The strength and elastic modulus along the printing direction were higher, while the strength perpendicular to the printing direction was lower.

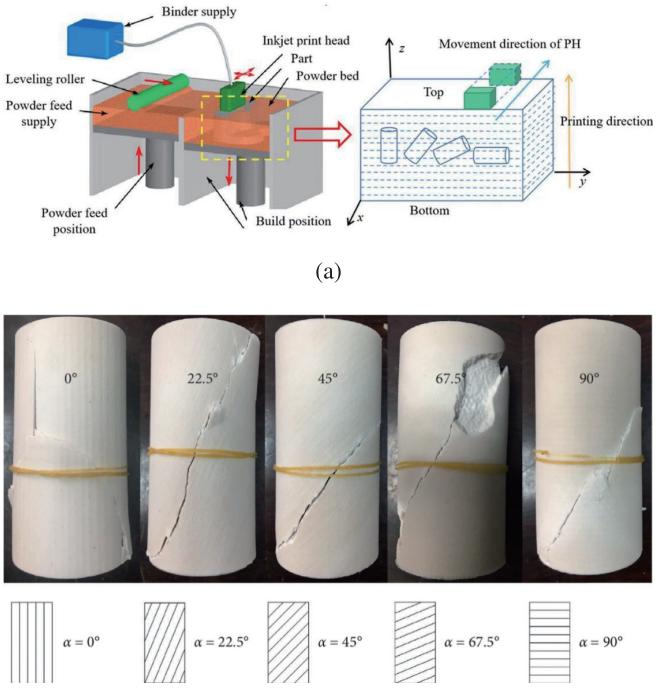

(a)

(b)

Fig. 7. (a) Printing schemes [77] and (b) failure patterns of printed samples with different printing orientations [78].

4. Postprocessing

Upon completion of the printing process, the fabricated specimen remains embedded in the uncured loose powder bed. The freshly printed specimen is highly porous and full of defects. It exhibits low density and mechanical strength. Therefore, after the printed specimen is removed from the powder bed, post-processing treatments, such as de-powdering, curing, and conditioning, are usually adopted to enhance structural and mechanical properties. The post-

processing methods could be infiltration, impregnation, or sintering according to the printing material.

4.1. Powder removal

Before powder removal, the printed component is typically left undisturbed within the powder bed for a certain period to develop sufficient forming strength, preventing damage during extraction due to incomplete curing. When removing excessive loose powder from the component surface, the method should be selected based on the complexity and internal features of printed specimens. For components without internal features, excessive powder can be removed using a brush, compressed air, or manual wiping, as shown in Fig. 8 [79]. In contrast, complex specimens or those with internal features may require additional steps, such as blowing, vacuuming, or vibration-based dry methods, as well as ultrasonic cleaning or microwave-induced boiling wet methods [80]. He et al. [81] utilized chemical polishing method with acetone vapor polishing to remove the stepped textures on the surface of the printed model, and finally obtained smooth and high-precision medical prosthesis. After powder removal, the component should be dried before undergoing further post-processing.

To avoid or minimize damage to large (meter-scale) BJ3DP raw embryos during powder removal, a comprehensive strategy is crucial. Design considerations should facilitate de-powdering access by including internal channels, reducing thin walls and overhangs, and considering part segmentation. Printing parameters must ensure sufficient binder saturation to enhance raw embryos strength. The powder removal process should be conducted gradually from top to bottom, using surrounding powder as natural support and employing gentle tools like low-pressure air and soft brushes. For large-sized components, custom fixtures or support structures are necessary to withstand self-weight and prevent deformation or fractures during handling. After de-powdering, handling should be minimized, and the part should be quickly transferred to subsequent processes such as curing, infiltration, or sintering to maximize integrity.

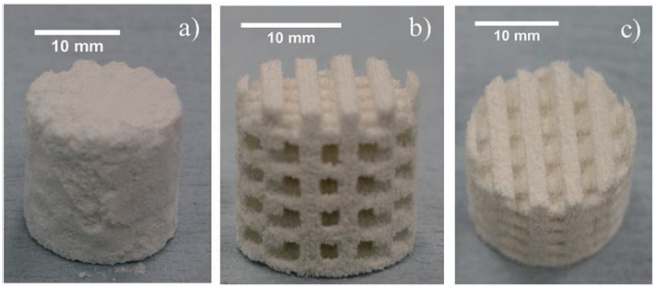

Fig. 8. (a) Printed model freshly removed from powder bed; (b-c) depowdered models [79].

4.2. Sintering

Sintering is another commonly post-processing technique to enhance the mechanical strength of binder jetting 3D printed specimens. During the sintering process, the printed component undergoes volumetric shrinkage, which reduces or even eliminates internal pores and defects to render dense specimens. Prior to sintering, the former preforms can be placed in containers with higher melting points to serve as fixatives. The main sintering parameters include material selection, particle size, sintering time and temperature [82]. Metals exhibit high sintering flexibility, allowing sintering behavior to be modified by adjusting particle distribution or incorporating metal mixtures [83]. The sintering behavior of ceramics is generally intricate to be modulated and sintering aids, such as tetraethyl orthosilicate, should be engaged to improve the sintering effect. Nan et al. [84] utilized BJ3DP to fabricate TiC-TiO_2 composite powder-based components, which were subsequently sintered under an inert atmosphere for secondary consolidation. Additionally, aluminum infiltration was employed to fill internal pores, further enhancing densification and mechanical properties.

4.3. Infiltration

Infiltration is a densification method that increases the density of printed components without significant shrinkage. The infiltrant penetrates internal pores via capillary action, thereby enhancing the mechanical properties of printed specimens. Both low-temperature and high-temperature infiltration processes can be employed, depending on the part material and bonding

mechanism. To achieve desired material properties, optimizing the saturation of infiltrant is crucial. Excessive infiltration compromises dimensional accuracy, whereas insufficient infiltration may result in insufficient solidification of the powder material, negating mechanical performance [85]. Molten infiltrant should exhibit sufficient fluidity and low viscosity, as well as low contact angle with printed specimens to ensure effective penetration. Low-temperature penetration is usually carried out at ambient temperature or slightly above ambient temperature, and the penetrant includes molten wax, varnish, etc. Xia et al. [48] improved the compressive strength of geopolymer-based printed specimens by immersing specimens in 60°C saturated anhydrous sodium metasilicate solution, increasing strength from 0.91 MPa to 16.5 MPa. Andrzej et al.[86] employed epoxy resin and silicone varnish impregnation to reinforce sand-based 3D printed specimens. As shown in Fig. 9, microstructure of the printed components assumes different states under different environmental temperatures, pressures, and immersion times. Specifically, impregnating with epoxy resin at 65°C for 5 minutes can effectively fill up micropores and defects. Polymer infiltration significantly enhances the mechanical properties of sand molds, especially increasing the flexural strength and impact resistance by more than 20 times and 5 times, respectively.

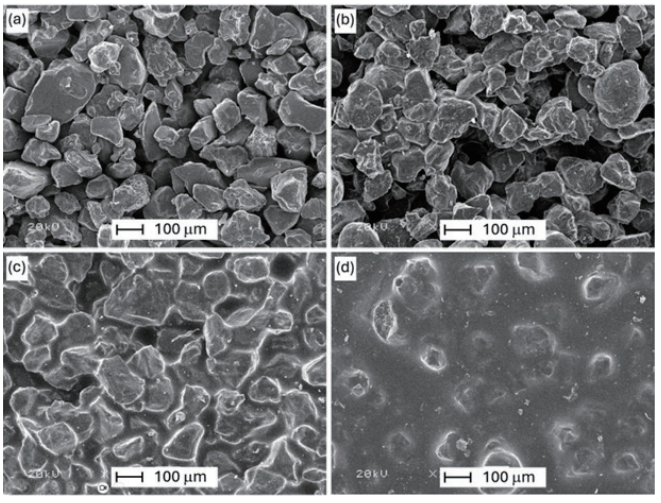

Fig. 9. (a) Unprocessed specimen; (b-d) specimens subject to different impregnation conditions [86].

5. Applications and challenges

5.1 Applications

Binder jetting 3D printing (BJ3DP) has demonstrated significant potential for extensive civil engineering applications. In architectural domains, BJ3DP has been employed to produce customized building components, formworks, molds, facade elements, and prefabricated construction units [29, 49, 87, 88]. Its viability for manufacturing complex geometries enables realization of intricate designs that are challenging, if not impossible, for conventional manufacturing methods. Wang et al. [89] revealed that calcium sulfoaluminate (CSA) cement containing rounded silica sand exhibited optimal mechanical properties and surface quality. Subsequently, lattice-structured components were successfully fabricated using self-developed CSA cementitious materials (Fig. 10(a)). As illustrated in Fig. 10(b), sand-based 3D printing technology has been frequently utilized for mold fabrication, typically employing refractory materials such as alumina cement and ceramsite. Enrico Dini [29] fabricated the Radiolaria Pavillon structure using magnesia sand, as shown in Fig.11. Binder jetting 3D printing technology has proven to be highly effective in printing very large-scale objects: for instance, it enables the construction of a lunar concrete wall or a complete house in a single printing process, as shown in Fig. 12. Fig. 13 shows a pedestrian bridge in Madrid's Castilla Park (2016) constructed using binder jetting 3D printing technology, where Portland cement and steel fibers were used in manufacturing bridge components that were subsequently assembled into the complete structure.

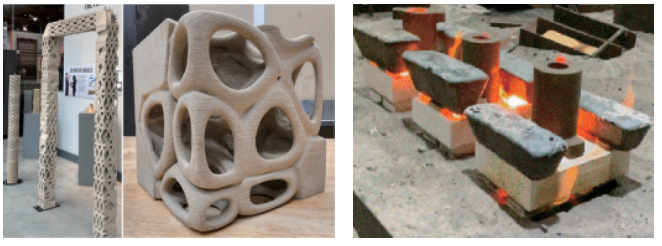

(a) (b)

Fig. 10. (a) Hollow artifacts [89]; (b) binder jetting 3D molds [49].

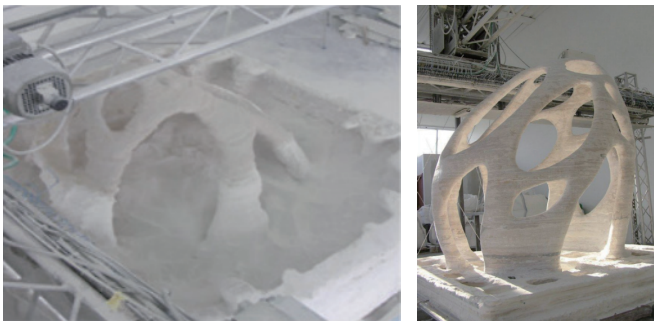

Fig. 11. Binder jetting 3D printed Radiolaria Pavillon [29].

(a) (b)

Fig. 12. (a) Lunar concrete of 1.5 ton printed using a regolith simulant and (b) a complete house printed in one single process [90].

(a)

(b)

Fig. 13. Binder jetting 3D printed footbridge in Madrid:(a) segments and (b) overall bridge [91].

The high-precision characteristics of binder jetting 3D printing (BJ3DP) have been leveraged to fabricate miniature complex models using materials of gypsum, inorganic polymer powders, and cement. The white coloration of gypsum enables full-color printing viability in BJ3DP gypsum models, facilitating the production of vibrantly colored prototypes. CONCR3DE employed BJ3DP technology with inorganic polymer powder to create coral-shaped lamp covers, where the hardened material exhibited sandstone-like appearance [92], as shown in Fig. 14(a). Xia et al. [93] designed and printed geometrically intricate opera house model using self-developed Portland cement (Fig. 14(b)), demonstrating viability for BJ3DP applications for complex geometries. Ma et al. [3] developed magnesium phosphate cement composite, comprising magnesium phosphate cement and basalt fibers, for manufacturing high-precision models. This composite material shows potential for fabricating thin-walled models of complex structures, as illustrated in Fig. 15.

(a) (b)

Fig. 14. (a) Lamp in coral shape [92] and (b) opera house model [93].

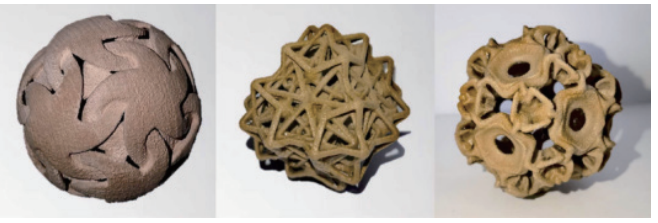

Fig. 15. Delicate hollow structures with complex details [3].

Furthermore, binder jetting 3D printing (BJ3DP) is increasingly employed for fabricating artificial rock and geological models. Gypsum powder was firstly adopted for fabrication of rock-like specimen. However, it yielded substantial property discrepancies from

those of natural rocks [94]. To enhance the mechanical strength of gypsum-printed specimens, researchers have implemented vacuum-assisted binder infiltration techniques, achieving uniaxial compressive strengths of 40-57 MPa. Nevertheless, gypsum-printed specimens retain notable ductility, making them suitable for simulating high-stress soft rocks only [95, 96]. Silica sand has been widely utilized for sandstone analog production due to its granular structure resembling that of natural sandstone [87, 97, 98]. However, organic binders employed in gypsum-based and sand-based printing tend to impart residual ductility to untreated specimens.

To address these limitations, adoption of inherently brittle cementitious materials as powder constituents in BJ3DP shows significant potential for manufacturing highly brittle and precision-controlled rock-like specimens [99-102]. Ma et al. [103] optimized printed specimen dimensional accuracy, mechanical performance, and anisotropy through parametric adjustments of layer thickness, molar ratios, and borax dosage, effectively approaching natural brittle rock characteristics. Regarding fracture fabrication, gypsum powder and silica sand remain predominant materials for fractured specimen construction [104-107]. However, application of cement in crack preparation is not so profuse. Nevertheless, as depicted in Fig. 16, Ma et al. [103] established a magnesium phosphate cement (MPC)-based BJ3DP system, successfully fabricating low-anisotropy brittle matrices and complex fractured rock analogs using proprietary printing equipment. As shown in Fig. 17, the MPC material has further demonstrated viability in reconstructing intricate geological canyon models, accurately replicating topographic features including canyons, river channels, and mountain peaks. The printed models exhibited dimensional errors of 1.25%, 0.78%, and 3.56% along the X, Y, and Z axes respectively relative to design specifications, suggesting high precision for complex geometries [102].

Binder Jetting 3D Printing (BJ3DP) has demonstrated significant potential in a wide range of civil engineering applications. In the construction sector, BJ3DP has been applied to produce customized architectural components, formworks, molds, façade elements, and prefabricated building units. Its viability to fabricate complex geometries enables construction of intricate designs that are not feasible to achieve with traditional methods. Moreover, BJ3DP is being increasingly used to fabricate artificial rocks and geological models, which are valuable for geotechnical and rock mechanics research. In infrastructure development, BJ3DP can be utilized for manufacturing lightweight structural components, drainage systems, and pavement structures with optimized internal configurations. Additionally, the use of eco-friendly materials such as geopolymer and recycled powders in BJ3DP contributes to the development of green construction.

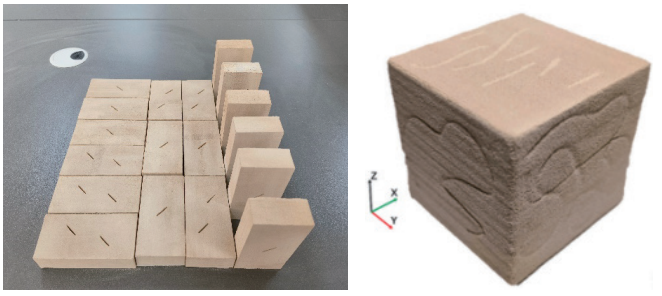

(a) (b)

Fig. 16. BJ 3D printed fractured specimens with cement:(a) 2D fracture and (b) complex fracture [103].

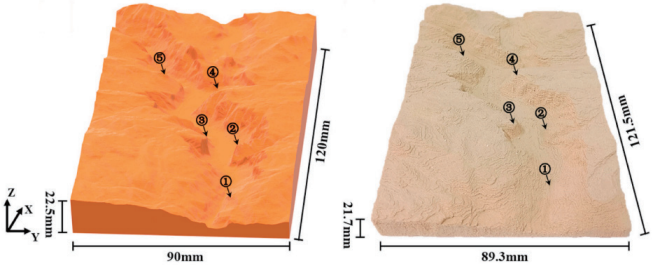

Fig. 17. Precision printing: complex geological canyon model [102].

5.2 Challenges and prospect

Despite its distinct advantages, several challenges persist to hinder the large-scale fabrication by BJ3DP in civil engineering applications, primarily due to the intricate interplay among material properties, process parameters, and post-processing requirements. Further investigation and optimization are expected to achieve large-scale, reproducible and high-quality printed

components. Still, BJ3DP technology holds significant promise for revolutionizing the field through synergistic innovations in material formulations, binder systems, and process engineering.

The diversification of material systems underscores a core research direction, encompassing the development of high-performance fiber-reinforced composites, nano-modified cementitious materials, recycled aggregates, and industrial waste-based sustainable construction materials. It collectively addresses diverse requirements for mechanical performance, durability, and functional adaptability across different application scenarios. Researches on binder prioritize functionalization and environmental sustainability, exemplified by the advancement of low-carbon binders utilizing biopolymers or geopolymers, alongside smart binders endowed with self-healing, conductive, or temperature-responsive properties to enable multifunctional printed components. Process innovation necessitates synergistic integration of multiscale precision control and intelligent production workflows, incorporating multi-nozzle coordinated jetting, gradient structural design, and real-time monitoring technologies. Machine learning-driven optimization of interlayer quality and dimensional accuracy, coupling with high-resolution nozzle technology and multi-material deposition methodologies, is expected to ultimately facilitate the efficient monolithic fabrication of complex freeform structures.

6. Conclusions

Binder jetting 3D printing has emerged as a transformative technology in civil engineering due to its high efficiency, cost-effectiveness, and viability for fabricating complex geometries. This technology utilizes layer-by-layer deposition and binder gluing mechanisms to precisely fabricate cement-based materials, sandy soils, and composites. These viabilities enable innovative production methods for customized building components, such as lightweight walls and porous sound-absorbing structures. Additionally, it supports irregular geometric designs, including curved bridges and biomimetic infrastructure systems. Currently available studies focus on material system development, revealing the influences of water-to-cement ratios, aggregate gradation, and binder dosage on the mechanical properties of printed components. Concurrently, optimization of process parameters, such as layer thickness, jetting speed, and curing conditions, has significantly improved dimensional accuracy and structural integrity. However, existing achievements are predominantly limited to laboratory-scale applications. Further systematic validation is required to assess the printing stability of large-scale components, interlayer bonding strength, and long-term durability under environmental conditions, including freeze-thaw cycles and corrosion. Moreover, the compatibility of multi-material collaborative printing and the structural response mechanisms under complex loading scenarios remain poorly understood, which hinders implementation of this technology in practical engineering applications. Future exploration in material innovation and process scalability are expected to bridge the gap between academic research and industrial applicability, fostering sustainable and intelligent construction practices.

Author credit statement

Tingyu Hu: Investigation, Analysis, Writing of original draft of the manuscript; Zhijian Li: Supervision, Methodology; Guowei Ma: Writing-reviewing and editing of the manuscript, Conceptualization, Funding acquisition.

References

[1] Kunchala, P., & Kappagantula, K. (2018). 3D printing high density ceramics using binder jetting with nanoparticle densifiers. Materials and Design, 155, 443-450.

[2] Park, K., Min, K., Lee, B., & Roh, Y. (2021). Proposal for enhancing the compressive strength of alkali-activated materials-based binder jetting 3D printed outputs. Construction and Building Materials, 303, 124377.

[3] Ma, G., Dou, C., Wang, L., Wang, F., & Li, Z. (2025). Mechanical improvement of basalt fiber reinforced cementitious material for binder jetting 3D printing. Additive Manufacturing, 100, 104688.

[4] Mariani, M., Beltrami, R., Brusa, P., Galassi, C., Ardito, R., & Lecis, N. (2021). 3D printing of fine alumina powders by binder jetting. Journal of the European Ceramic Society, 41(10), 5307-5315.

[5] Bui, H.M., Fischer, R., Szesni, N., Tonigold, M., Achterhold, K., Pfeiffer, F., & Hinrichsen, O. (2022). Development of a manufacturing process for Binder Jet 3D printed porous Al2O3 supports used in heterogeneous catalysis. Additive Manufacturing, 50, 102498.

[6] Salari, F., Bosetti, P., & Sglavo, V.M. (2022). Binder Jetting 3D Printing of Magnesium Oxychloride Cement-Based Materials: Parametric Analysis of Manufacturing Factors, Journal of Manufacturing and Materials Processing, 6, 86.

[7] Ngo, T.D., Kashani, A., Imbalzano, G., Nguyen, K.T.Q., & Hui, D. (2018). Additive manufacturing (3D printing): A review of materials, methods, applications and challenges. Composites Part B: Engineering, 143, 172-196.

[8] Kanwar, S., & Vijayavenkataraman, S. (2021). Design of 3D printed scaffolds for bone tissue engineering: A review. Bioprinting, 24, e00167.

[9] Godoi, F.C., Prakash, S., & Bhandari, B.R. (2016). 3d printing technologies applied for food design: Status and prospects. Journal of Food Engineering, 179, 44-54.

[10] Lowke, D., Talke, D., Dressler, I., Weger, D., Gehlen, C., Ostertag, C., & Rael, R. (2020). Particle bed 3D printing by selective cement activation – Applications, material and process technology. Cement and Concrete Research, 134, 106077.

[11] Yin, Y., Huang, J., Wang, T., Yang, R., Hu, H., Manuka, M., Zhou, F., Min, J., Wan, H., Yuan, D., & Ma, B. (2023). Effect of Hydroxypropyl methyl cellulose (HPMC) on rheology and printability of the first printed layer of cement activated slag-based 3D printing concrete. Construction and Building Materials, 405, 133347.

[12] Xia, M., Nematollahi, B., & Sanjayan, J. (2019). Printability, accuracy and strength of geopolymer made using powder-based 3D printing for construction applications. Automation in Construction, 101, 179-189.

[13] Rajeev, P., Ramesh, A., Navaratnam, S., & Sanjayan, J. (2023). Using Fibre recovered from face mask waste to improve printability in 3D concrete printing. Cement and Concrete Composites, 139, 105047.

[14] Voney, V., Odaglia, P., Brumaud, C., Dillenburger, B., & Habert, G. (2021). From casting to 3D printing geopolymers: A proof of concept. Cement and Concrete Research, 143, 106374.

[15] Sivarupan, T., Balasubramani, N., Saxena, P., Nagarajan, D., El Mansori, M., Salonitis, K., Jolly, M., & Dargusch, M.S. (2021). A review on the progress and challenges of binder jet 3D printing of sand moulds for advanced casting. Additive Manufacturing, 40, 101889.

[16] Shahid, M., & Sglavo, V.M. (2024). Effect of water-to-quick setting cement ratio and aggregate size on mechanical properties and dimensional accuracy of binder jetting 3D-printed bodies. Open Ceramics, 20, 100704.

[17] Muthukrishnan, S., Ramakrishnan, S., & Sanjayan, J. (2022). Set on demand geopolymer using print head mixing for 3D concrete printing. Cement and Concrete Composites, 128, 104451.

[18] Zhu, S., Vazquez Ramos, P., Heckert, O.R., Stieger, M., van der Goot, A.J., & Schutyser, M. (2022). Creating protein-rich snack foods using binder jet 3D printing. Journal of Food Engineering, 332, 111124.

[19] Chen, Y., Jansen, K., Zhang, H., Romero Rodriguez, C., Gan, Y., Çopuroğlu, O., & Schlangen, E. (2020). Effect of printing parameters on interlayer bond strength of 3D printed limestone-calcined clay-based cementitious materials: An experimental and numerical study. Construction and Building Materials, 262, 120094.

[20] Huang, X., Yang, W., Song, F., & Zou, J. (2022). Study on the mechanical properties of 3D printing concrete layers and the mechanism of influence of printing parameters. Construction and Building Materials, 335, 127496.

[21] Shakor, P., Chu, S.H., Puzatova, A., & Dini, E. (2022). Review of binder jetting 3D printing in the construction industry. Progress in Additive Manufacturing, 7(4), 643-669.

[22] Sen, K., Mehta, T., Sansare, S., Sharifi, L., Ma, A.W.K., & Chaudhuri, B. (2021). Pharmaceutical applications of powder-based binder jet 3D printing process – A review. Advanced Drug Delivery Reviews, 177, 113943.

[23] Nandwana, P., Elliott, A.M., Siddel, D., Merriman, A., Peter, W.H., & Babu, S.S. (2017). Powder bed binder jet 3D printing of Inconel 718: Densification, microstructural evolution and challenges ☆ . Current Opinion in Solid State and Materials Science, 21(4), 207-218.

[24] Chen, X., Wang, S., Wu, J., Duan, S., Wang, X., Hong, X., Han, X., Li, C., Kang, D., Wang, Z., & Zheng, A. (2022). The Application and Challenge of Binder Jet 3D Printing Technology in Pharmaceutical Manufacturing, Pharmaceutics, 14(12), 2589.

[25] Bong, S.H., Xia, M., Nematollahi, B., & Shi, C. (2021). Ambient temperature cured 'just-add-water' geopolymer for 3D concrete printing applications. Cement and Concrete Composites, 121, 104060.

[26] Ma, G., Hu, T., & Li, Z. (2024). Binder jetting 3D printing rock analogs using magnesium phosphate cement. Construction and Building Materials, 420, 135620.

[27] Ma, G., Hu, T., Wang, F., Liu, X., & Li, Z. (2023). Magnesium phosphate cement for powder-based 3D concrete printing: Systematic evaluation and optimization of printability and printing quality. Cement and Concrete Composites, 139, 105000.

[28] Voney, V., Odaglia, P., Brumaud, C., Dillenburger, B., & Habert, G., Geopolymer Formulation for Binder Jet 3D Printing, in: F.P. Bos, S.S. Lucas, R.J.M. Wolfs, & T.A.M. Salet (Eds.) Second RILEM International Conference on Concrete and Digital Fabrication, Springer International Publishing, Cham, 2020, pp. 153-161.

[29] Lowke, D., Dini, E., Perrot, A., Weger, D., Gehlen, C., & Dillenburger, B. (2018). Particle-bed 3D printing in concrete construction – Possibilities and challenges. Cement and Concrete Research, 112, 50-65.

[30] Meibodi, M.A., Bernhard, M., Jipa, A., Dillenburger, B., Menges, A., Sheil, B.O.B., Glynn, R., & Skavara, M. (2017). The smart takes from the strong: 3D printing stay-in-place formwork for concrete slab construction, Fabricate 2017, UCL Press, 210-217.

[31] Dini, F., Ghaffari, S.A., Jafar, J., Hamidreza, R., & Marjan, S. (2020). A review of binder jet process parameters; powder, binder, printing and sintering condition. Metal Powder Report, 75(2), 95-100.

[32] Shahid, M., & Sglavo, V.M. (2024). Binder Jetting 3D Printing of Binary Cement—Siliceous Sand Mixture, Materials, 17(7), 1514.

[33] Na, O., Kim, K., Lee, H., & Lee, H. (2021). Printability and Setting Time of CSA Cement with Na2SiO3 and Gypsum for Binder Jetting 3D Printing, Materials, 14, 2811.

[34] Liu, J., Li, P., Jin, D., Her, S., Kim, J., Yoon, Y., Baldassari, M., & Bae, S. (2023). Evaluation of the mechanical and photocatalytic properties of TiO2-reinforced cement-based materials in binder jet 3D printing. Journal of Building Engineering, 72, 106618.

[35] Shakor, P., Nejadi, S., Paul, G., & Sanjayan, J. (2020). Dimensional accuracy, flowability, wettability, and porosity in inkjet 3DP for gypsum and cement mortar materials. Automation in Construction, 110, 102964.

[36] Upadhyay, M., Sivarupan, T., & El Mansori, M. (2017). 3D printing for rapid sand casting—A review. Journal of Manufacturing Processes, 29, 211-220.

[37] Tan, J.H., Wong, W.L.E., & Dalgarno, K.W. (2017). An overview of powder granulometry on feedstock and part performance in the selective laser melting process. Additive Manufacturing, 18, 228-255.

[38] Zhou, Z., Buchanan, F., Mitchell, C., & Dunne, N. (2014). Printability of calcium phosphate: Calcium sulfate powders for the application of tissue engineered bone scaffolds using the 3D printing technique. Materials Science and

Engineering: C, 38, 1-10.
[39] Schade, C.T., Murphy, T.F., & Walton, C., Development of atomized powders for additive manufacturing, Powder Metallurgy Word Congress, Accessed on 2nd July, 2014.
[40] Chen, H., Wei, Q., Wen, S., Li, Z., & Shi, Y. (2017). Flow behavior of powder particles in layering process of selective laser melting: Numerical modeling and experimental verification based on discrete element method. International Journal of Machine Tools and Manufacture, 123, 146-159.
[41] Fonseca Coelho, A.W., da Silva Moreira Thiré, R.M., & Araujo, A.C. (2019). Manufacturing of gypsum–sisal fiber composites using binder jetting. Additive Manufacturing, 29, 100789.
[42] Ding, X., Shan, Z., Long, Z., & Chen, Z. (2020). Utilization of collagen protein extracted from chrome leather scraps as a set retarders in gypsum. Construction and Building Materials, 237, 117584.
[43] Ma, B., Jiang, Q., Huang, J., Wang, X., & Leng, J. (2019). Effect of different silica particles on flowability of gypsum powder for 3D powder printing. Construction and Building Materials, 217, 394-402.
[44] Kong, L., Ostadhassan, M., Li, C., & Tamimi, N.J.J.o.m.s. (2018). Pore characterization of 3D-printed gypsum rocks: a comprehensive approach. 53, 5063-5078.
[45] Kong, L., Ostadhassan, M., Liu, B., Li, C., & Liu, K.J.T.i.p.m. (2019). Multifractal characteristics of MIP-based pore size distribution of 3D-printed powder-based rocks: a study of post-processing effect. 129, 599-618.
[46] Jiang, Q., Liu, X., Yan, F., Yang, Y., Xu, D., Feng, G.J.R.M., & Engineering, R. (2021). Failure performance of 3DP physical twin-tunnel model and corresponding safety factor evaluation. 54, 109-128.
[47] Xia, M., Nematollahi, B., & Sanjayan, J. (2018). Influence of binder saturation level on compressive strength and dimensional accuracy of powder-based 3D printed geopolymer, Materials science forum, Trans Tech Publ, 939, 177-183.
[48] Xia, M., & Sanjayan, J. (2016). Method of formulating geopolymer for 3D printing for construction applications. Materials and Design, 110, 382-390.
[49] Chun, S., Kim, S., Kim, W., Lee, G., Lee, M., Ye, B., Kim, H., Lee, J.H., & Kim, T. (2023). Powder-bed-based 3D printing with cement for sustainable casting. Journal of Materials Research and Technology, 22, 3192-3206.
[50] Xu, J., Chen, M., Zhao, Z., Li, L., Wang, S., Huang, Y., Zhao, P., Gong, C., Lu, L., & Cheng, X. (2021). Printability and efflorescence control of admixtures modified 3D printed white Portland cement-based materials based on the response surface methodology. Journal of Building Engineering, 38, 102208.
[51] Na, O., Kim, K., Lee, H., & Lee, H.J.M. (2021). Printability and setting time of CSA cement with Na2SiO3 and gypsum for binder jetting 3D printing. 14(11), 2811.
[52] Shakor, P., Sanjayan, J., Nazari, A., & Nejadi, S. (2017). Modified 3D printed powder to cement-based material and mechanical properties of cement scaffold used in 3D printing. Construction and Building Materials, 138, 398-409.
[53] Ingaglio, J., Fox, J., Naito, C.J., Bocchini, P.J.C., & Materials, B. (2019). Material characteristics of binder jet 3D printed hydrated CSA cement with the addition of fine aggregates. 206, 494-503.
[54] Pegna, J. (1995). Application of Cementitious Bulk materials to Site Processed Solid Freeform Construction. Mechanical Engineering, 45 (9), 176-182. .
[55] V, C., & D, E. (2013). Large scale 3D printing: From Deep Sea to the Moon, in "low-cost 3D printing for science, education and sustainable development. ICTP - The Abdus Salam Centre for Theoretical Physics, ICTP Science Dissemination Unit, 127-132.
[56] Jazayeri, H.E., Rodriguez-Romero, M., Razavi, M., Tahriri, M., Ganjawalla, K., Rasoulianboroujeni, M., Malekoshoaraie, M.H., Khoshroo, K., & Tayebi, L. (2018). The cross-disciplinary emergence of 3D

printed bioceramic scaffolds in orthopedic bioengineering. Ceramics International, 44(1), 1-9.

[57] Zocca, A., Colombo, P., Gomes, C.M., Günster, J., & Green, D.J. (2015). Additive Manufacturing of Ceramics: Issues, Potentialities, and Opportunities. Journal of the American Ceramic Society, 98(7), 1983-2001.

[58] Colombo, P., Mera, G., Riedel, R., & Sorarù, G.D. (2010). Polymer - Derived Ceramics: 40 Years of Research and Innovation in Advanced Ceramics. Journal of the American Ceramic Society, 93(7), 1805-1837.

[59] Teng, W.D., Edirisinghe, M.J., & Evans, J.R.G. (2005). Optimization of Dispersion and Viscosity of a Ceramic Jet Printing Ink. Journal of the American Ceramic Society, 80(2), 486-494.

[60] Du, W., Ren, X., Ma, C., & Pei, Z. (2017). Binder jetting additive manufacturing of ceramics: A literature review, ASME international mechanical engineering congress and exposition, American Society of Mechanical Engineers, 58493, V014T07A006.

[61] Gonzalez, J.A., Mireles, J., Lin, Y., & Wicker, R.B. (2016). Characterization of ceramic components fabricated using binder jetting additive manufacturing technology. Ceramics International, 42(9), 10559-10564.

[62] Marczyk, J., & Hebda, M. (2023). Effect of the Particle Size Distribution of Irregular Al Powder on Properties of Parts for Electronics Fabricated by Binder Jetting. Electronics, 12(12), 2733.

[63] Voxeljet Presents cold IOB 3D Printing Tech at GIFA 2023, https://www.engineering.com/voxeljet-presents-cold-iob-3d-printing-tech-at-gifa-2023/ (accessed 08 Jun 2025).

[64] Amend, P., Pscherer, C., Rechtenwald, T., Frick, T., & Schmidt, M. (2010). A fast and flexible method for manufacturing 3D molded interconnect devices by the use of a rapid prototyping technology. Physics Procedia, 5, 561-572.

[65] Del Giudice, L., & Vassiliou, M.F. (2020). Mechanical properties of 3D printed material with binder jet technology and potential applications of additive manufacturing in seismic testing of structures. Additive Manufacturing, 36, 101714.

[66] Lu, K., Hiser, M., & Wu, W. (2009). Effect of particle size on three dimensional printed mesh structures. Powder Technology, 192(2), 178-183.

[67] Butscher, A., Bohner, M., Roth, C., Ernstberger, A., Heuberger, R., Doebelin, N., Rudolf von Rohr, P., & Müller, R. (2012). Printability of calcium phosphate powders for three-dimensional printing of tissue engineering scaffolds. Acta Biomaterialia, 8(1), 373-385.

[68] Mostafaei, A., Rodriguez De Vecchis, P., Nettleship, I., & Chmielus, M. (2019). Effect of powder size distribution on densification and microstructural evolution of binder-jet 3D-printed alloy 625. Materials & Design, 162, 375-383.

[69] Bae, M.A., Kim, K.H., & Baek, J.H. (2023). Effect of the Properties of Binder and Powder Used in Binder Jet 3D Printing on Build-Up. International Journal of Metalcasting, 17(4), 2500-2507.

[70] Chen, H., & Zhao, Y.F. (2016). Process parameters optimization for improving surface quality and manufacturing accuracy of binder jetting additive manufacturing process. Rapid Prototyping Journal, 22(3), 527-538.

[71] Mostafaei, A., Elliott, A.M., Barnes, J.E., Li, F., Tan, W., Cramer, C.L., Nandwana, P., & Chmielus, M. (2021). Binder jet 3D printing—Process parameters, materials, properties, modeling, and challenges. Progress in Materials Science, 119, 100707.

[72] Shrestha, S., & Manogharan, G. (2017). Optimization of Binder Jetting Using Taguchi Method. Jom, 69(3), 491-497.

[73] Y, S., E, T., & C, W. (2007). Modeling and characterization of biomaterials spreading properties in powder-based rapid prototyping techniques Yaser. In: Proc IMECE2007, pp, 135-143.

[74] Miyanaji, H., Momenzadeh, N., & Yang, L. (2018). Effect of printing speed on quality of printed parts in Binder Jetting Process. Additive

Manufacturing, 20, 1-10.
[75] Vaezi, M., & Chua, C.K. (2010). Effects of layer thickness and binder saturation level parameters on 3D printing process. The International Journal of Advanced Manufacturing Technology, 53(1-4), 275-284.
[76] AC, H., & HJ, F. (1995). A relation for the void fraction of randomly packed particle beds Powder Technology, 82, 197–203.
[77] Shao, Y., Yang, J., Kim, J., Song, J.-J., Moon, J., & Han, J. (2023). A Comprehensive Experimental Study on Mechanical Anisotropy and Failure Mode of 3D Printed Gypsum Rocks: From Composition and Microstructure to Macroscopic Mechanical Properties Response. Rock Mechanics and Rock Engineering, 56(9), 6503-6528.
[78] He, F., Liu, Q., Deng, P., & Aizenshtein, M. (2020). Investigation of the Anisotropic Characteristics of Layered Rocks under Uniaxial Compression Based on the 3D Printing Technology and the Combined Finite - Discrete Element Method. Advances in Materials Science and Engineering, 1, 8793214.
[79] Cox, S.C., Thornby, J.A., Gibbons, G.J., Williams, M.A., & Mallick, K.K. (2015). 3D printing of porous hydroxyapatite scaffolds intended for use in bone tissue engineering applications. Materials Science and Engineering: C, 47, 237-247.
[80] Bai, Y., & Williams, C.B. (2018). Binder jetting additive manufacturing with a particle-free metal ink as a binder precursor. Materials and Design, 147, 146-156.
[81] He, Y., Xue, G.-h., & Fu, J.-z. (2014). Fabrication of low cost soft tissue prostheses with the desktop 3D printer. Scientific Reports, 4(1), 6973.
[82] Utela, B., Storti, D., Anderson, R., & Ganter, M. (2008). A review of process development steps for new material systems in three dimensional printing (3DP). Journal of Manufacturing Processes, 10(2), 96-104.
[83] R, F., Y, T., B-G, A., & R, C. (2016). Solid state sintered 3-D printing component by using Inkjet (Binder) Method. Journal of the Japan Society of Powder and Powder Metallurgy, 63, 421–426.
[84] Nan, B., Yin, X., Zhang, L., & Cheng, L. (2011). Three-Dimensional Printing of Ti3SiC2-Based Ceramics. Journal of the American Ceramic Society, 94(4), 969-972.
[85] Fayazfar, H., Salarian, M., Rogalsky, A., Sarker, D., Russo, P., Paserin, V., & Toyserkani, E. (2018). A critical review of powder-based additive manufacturing of ferrous alloys: Process parameters, microstructure and mechanical properties. Materials and Design, 144, 98-128.
[86] Rybak, A., Javora, R., Sekula, R., & Kmita, G. (2024). The Influence of Polymer Impregnating Materials on Structural Strengthening of 3D Printed Sand Molds Produced by Binder Jetting Method. Polymers, 16(21), 2978.
[87] Wang, F., Cui, X., Yang, Q., Song, H., & Li, D. (2023). Fabrication and posttreatment for inorganic binder jetting sand molds for casting. Additive Manufacturing, 73, 103690.
[88] Walker, J., Harris, E., Lynagh, C., Beck, A., Lonardo, R., Vuksanovich, B., Thiel, J., Rogers, K., Conner, B., & MacDonald, E. (2018). 3D Printed Smart Molds for Sand Casting. International Journal of Metalcasting, 12(4), 785-796.
[89] Wang, X., Naito, C., Fox, J.T., & Bocchini, P. (2024). Impact of mix proportions on particle bed 3D printed concrete properties. Construction and Building Materials, 419, 135441.
[90] Cesaretti, G., Dini, E., De Kestelier, X., Colla, V., & Pambaguian, L. (2014). Building components for an outpost on the Lunar soil by means of a novel 3D printing technology. Acta Astronautica, 93, 430-450.
[91] de la Fuente, A., Blanco, A., Galeote, E., & Cavalaro, S. (2022). Structural fibre-reinforced cement-based composite designed for particle bed 3D printing systems. Case study Parque de Castilla Footbridge in Madrid. Cement and Concrete Research, 157, 106801.
[92] CONCR3DE|High End Sustainable 3D Printing, http://concr3de.com/ (accessed 20 March 2025).
[93] Xia, M., Nematollahi, B., & Sanjayan, J. (2019). Compressive strength and dimensional accuracy of portland cement mortar made using powder-

based 3D printing for construction applications, First RILEM International Conference on Concrete and Digital Fabrication–Digital Concrete 2018, Springer, pp. 245-254.

[94] Fereshtenejad, S., & Song, J.J. (2016). Fundamental study on applicability of powder-based 3d printer for physical modeling in rock mechanics. Rock Mechanics and Rock Engineering, 49(6), 2065-2074.

[95] Wu, Z., Zhang, B., Weng, L., Liu, Q., & Wong, L. (2019). A New Way to Replicate the Highly Stressed Soft Rock: 3D Printing Exploration. Rock Mechanics and Rock Engineering, 53, 467-476.

[96] Shao, Y., Kim, J., Yang, J., Song, J.-J., & Moon, J. (2024). Experimental Study on Strength Enhancement and Porosity Variation of 3D-Printed Gypsum Rocks: Insights on Vacuum Infiltration Post-Processing. Rock Mechanics and Rock Engineering, 57(9), 6763-6786.

[97] Hodder, K.J., Nychka, J.A., & Chalaturnyk, R.J. (2018). Improvement of the unconfined compressive strength of 3D-printed model rock via silica sand functionalization using silane coupling agents. International Journal of Adhesion and Adhesives, 85, 274-280.

[98] Zhang, K., Zhang, K., Jin, K., Hu, K., & Xie, J. (2023). Influence of intermittent opening density on mechanical behavior and fracture characteristics of 3D-printed rock. Theoretical and Applied Fracture Mechanics, 124, 103764.

[99] Bilginer, B.A., & Erdoğan, S.T. (2021). Effect of mixture proportioning on the strength and mineralogy of magnesium phosphate cements. Construction and Building Materials, 277, 122264.

[100] Qin, J., Dai, F., Ma, H., Dai, X., Li, Z., Jia, X., & Qian, J. (2022). Development and characterization of magnesium phosphate cement based ultra-high performance concrete. Composites Part B: Engineering, 234, 109694.

[101] Cao, X., & Li, Z., Factors influencing the mechanical properties of three-dimensional printed products from magnesium potassium phosphate cement material, 3D Concrete Printing Technology, Elsevier Inc., 2019, pp. 211-222.

[102] Ma, G., Hu, T., Wang, F., Liu, X., & Li, Z. (2023). Magnesium phosphate cement for powder-based 3D concrete printing: Systematic evaluation and optimization of printability and printing quality. Cement and Concrete Composites, 139, 105000.

[103] Ma, G., Hu, T., & Li, Z. (2024). Binder jetting 3D printing rock analogs using magnesium phosphate cement. Construction and Building Materials, 420, 135620.

[104] Sharafisafa, M., & Shen, L. (2020). Experimental investigation of dynamic fracture patterns of 3D printed rock-like material under impact with digital image correlation. Rock Mechanics and Rock Engineering, 53(8), 3589-3607.

[105] Zhao, Y., Jiang, L., Li, C., Niu, Q., Sainoki, A., Mitri, H.S., & Ning, J. (2023). Experimental Investigation into the Mechanical Behavior of Jointed Soft Rock Using Sand Powder 3D Printing. Rock Mechanics and Rock Engineering, 1-22.

[106] Liu, X., Pan, Z., Wang, J., Hu, Q., Xiong, W., & Zhang, K. (2023). Quantitative investigation of the cracking mechanism of 3D sand-printed rock containing a fold flaw. Materials and Design, 236, 112523.

[107] Yu, C., Tian, W., Zhang, C., Chai, S., Cheng, X., & Wang, X. (2021). Temperature-dependent mechanical properties and crack propagation modes of 3D printed sandstones. International Journal of Rock Mechanics and Mining Sciences, 146, 104868.